

The nature of the chemical bond in $\text{BeO}^{0,-}$, $\text{BeOBe}^{+,0,-}$, and in their hydrogenated products $\text{HBeO}^{0,-}$, BeOH , HBeOH , $\text{BeOBeH}^{+,0,-}$, and HBeOBeH

Apostolos Kalamos

Citation: *The Journal of Chemical Physics* **146**, 104307 (2017); doi: 10.1063/1.4977930

View online: <http://dx.doi.org/10.1063/1.4977930>

View Table of Contents: <http://aip.scitation.org/toc/jcp/146/10>

Published by the *American Institute of Physics*



**COMPLETELY
REDESIGNED!**

Physics Today Buyer's Guide
Search with a purpose.

The nature of the chemical bond in $\text{BeO}^{0,-}$, $\text{BeOBe}^{+,0,-}$, and in their hydrogenated products $\text{HBeO}^{0,-}$, BeOH , HBeOH , $\text{BeOBeH}^{+,0,-}$, and HBeOBeH

Apostolos Kalamos^{a)}

Department of Chemistry, Laboratory of Physical Chemistry, National and Kapodistrian University of Athens, Panepistimiopolis, Athens 157 01, Greece

(Received 10 January 2017; accepted 21 February 2017; published online 14 March 2017)

The nature of the chemical bond in $\text{BeO}^{0,-}$, $\text{BeOBe}^{+,0,-}$, and in their hydrogenated products $\text{HBeO}^{0,-}$, BeOH , HBeOH , $\text{BeOBeH}^{+,0,-}$, and HBeOBeH has been studied through single and multi reference correlation methods. In all these species, excited and ionized atomic states participate in a resonant way making chemically possible molecules that have been termed hypervalent and explain also the “incompatible” geometrical structure of some species. *Published by AIP Publishing.* [<http://dx.doi.org/10.1063/1.4977930>]

I. INTRODUCTION

Even though the BeOBe species is composed of three simple and light atoms, it is usually termed as hypermetallic, hyperstoichiometric, or to put it simpler as a hypervalent molecule. It should not exist based on the current theory of valence, but since it defies the “traditional” rules of chemistry we should find out what is wrong with them, most importantly how this molecule is formed.

The story of the $\text{BeOBe}^{0,+}$ compounds is not old but highly intriguing and is well exposed in a recent frontiers article by Heaven and his collaborators.¹ It was first detected in mass spectrometric Knudsen effusion experiments by Theard and Hildenbrand in 1964.² Some thirty years later, Thompson and Andrews³ and Andrews *et al.*⁴ observed beryllium oxygen molecules in IR matrix isolation experiments. The latest experimental work on both neutral and cationic species was recently conducted by Heaven’s group through laser–induced fluorescence and resonance enhanced multiphoton ionization (BeOBe)⁵ and pulsed–field ionization zero electron kinetic energy photoelectron (BeOBe^+)⁶ techniques. What we know experimentally is that the neutral BeOBe system has a linear ground state of $\tilde{X}^1\Sigma_g^+$ symmetry with $r_e(\text{BeO}) = 1.396(3)$ Å, ground state vibrational frequencies of 1039 (σ_g^+), 1414 (σ_u^+), and 113 (π_u) cm^{-1} , and an ionization energy (IE) of $\text{IE} = 65\,480(4)$ cm^{-1} ($=8.118$ eV).^{5,6} The ground state of BeOBe^+ is of $\tilde{X}^2\Sigma_g^+$ symmetry with $r_e(\text{BeO}) = 1.392(8)$ Å, $\omega_e(\pi_u) = 151.1(4)$ cm^{-1} , $\omega_e x_e(\pi_u) = 3.5(1)$ cm^{-1} , and $\Delta G_{1/2} = 1037(4)$ (σ_g^+) and 144.2(5) (π_u) cm^{-1} .⁶ *Ab initio* calculations^{5,7} are in good agreement with the available experimental values and unanimously conclude on the multireference character of the ground state’s wavefunction dominated by two configurations responsible for 54% and 41% of the total density.

But it is the work of Boldyrev and Simons⁸ that addressed the major issues of the nature of the chemical bond in both BeO

and BeOBe . In particular, they attributed the strong binding in BeOBe to the ionic nature of Be^+O^- and studied its “double” bond by comparing its characteristics to a single BeO bond as the one found in HBeO , BeOH , and HBeOH . They concluded that BeO does not possess a conventional double bond and that the triatomic BeOBe system can be described as $\text{Be}^+\text{O}^{2-}\text{Be}^+$ with unpaired electrons localized on Be. The interesting question of a dative or double bond between O and other atoms was also recently discussed in Ref. 9. But the question of how this triatomic is formed is still an open issue. How a closed shell diatomic (BeO) forms such a strong bond with another closed shell atom (Be) and why a multireference closed shell triatomic (BeOBe , $\tilde{X}^1\Sigma_g^+$) is practically degenerate with a single reference open shell state ($\tilde{a}^3\Sigma_u^+$) being its first excited one?

In the present work we thoroughly studied the $\text{BeO}^{0,-}$ and $\text{BeOBe}^{+,0,-}$ species along with their hydrogenated products, $\text{HBeO}^{0,-}$, BeOH , HBeOH , $\text{BeOBeH}^{+,0,-}$, and HBeOBeH with the sole goal to understand the way all these species are formed. To this end we employed single reference or multireference (MR) configuration interaction (CI) and coupled cluster (CC) correlation methods in conjunction with the aug–cc–pVQZ basis set.¹⁰ The active space of the zeroth order wavefunction in our MR treatment is based on the plain valence space of the constituent atoms. All calculations have been performed with MOLPRO.¹¹

II. RESULTS AND DISCUSSION

We will first deal with the diatomics $\text{BeO}^{0,-}$ that provide the key to unlock the electronic and geometric “secrets” of $\text{HBeO}^{0,-}$, BeOH , and HBeOH . Finally, we will present the triatomics $\text{BeOBe}^{+,0,-}$ and then their hydrogenated products $\text{BeOBeH}^{+,0,-}$ and HBeOBeH and discuss the way all these “hyperstoichiometric” molecules are formed. The above species provide also a nice occasion to discuss on the validity and extension of the traditional rules of valence in order to understand molecular formation beyond the seeming limitations of the octet rule.

^{a)}kalamos@chem.uoa.gr

The most recent work on the neutral BeO species that we are aware of is a paper in 2000 by Sorensen and England¹² where a wealth of information can be found. For reasons of completeness and coherency we have studied its valence states whose potential energy curves (PEC) are displayed in Figure 1 while the usual molecular constants of the lowest ones are gathered in Table I. We have constructed PECs for 35 molecular states of singlet (10 states), triplet (18 states), and quintet (7 states) spin multiplicity dissociating to Be(¹S) + O(³P, ¹D, ¹S) and Be(³P) + O(³P, ¹D).

Its ground state is of $X^1\Sigma^+$ symmetry and dissociates adiabatically to the first excited asymptotic channel Be(¹S) + O(¹D). It is important to mention that the Hartree–Fock (HF) description of the O(¹D, M = 0) atom is given by

$$|{}^1D, M = 0\rangle = \frac{1}{\sqrt{6}} [2|2p_x^2 2p_y^2\rangle - |2p_x^2 2p_z^2\rangle - |2p_y^2 2p_z^2\rangle],$$

so it becomes pretty obvious that in the case of any bond formation with the Be(¹S) atom the second and third determinants should somehow disappear. Paradoxically enough, this does not happen as evidenced by the equilibrium CASSCF configurations (only valence e^- are shown),

$$|X^1\Sigma^+\rangle \cong 0.77|1\sigma^2 2\sigma^2 1\pi_x^2 1\pi_y^2\rangle + 0.38|1\sigma^2 2\sigma^2 (1\pi_x^2 1\pi_y^1 2\bar{\pi}_y^1 + 1\pi_x^1 2\bar{\pi}_x^1 1\pi_y^2)\rangle - 0.30|1\sigma^2 2\sigma^1 3\bar{\sigma}^1 1\pi_x^2 1\pi_y^2\rangle,$$

that mirror the characteristics of the above O wavefunction and where $1\sigma \cong 2s(\text{O})$, $2\sigma \cong 0.48 \times 2s(\text{Be}) + 0.50 \times 2p_z(\text{Be}) - 0.93 \times 2p_z(\text{O})$, $3\sigma \cong 0.76 \times 2s(\text{Be}) - 0.55 \times 2p_z(\text{Be})$, $1\pi \cong 2p_\pi(\text{O})$, and $2\pi \cong 2p_\pi(\text{Be})$. In order to understand the chemical pattern, it is crucial to mention the Mulliken atomic populations $2s^{0.32} 2p_z^{0.14} 2p_x^{0.37} 2p_y^{0.37} /_{\text{Be}} 2s^{1.89} 2p_z^{1.61} 2p_x^{1.59} 2p_y^{1.59} /_{\text{O}}$ ($q_{\text{Be}} = +0.76$) revealing a key element to the whole discussion. The very large negative charge accumulated on the O atom along with the very large dipole moment ($\mu = 5.9$ D) points to a state diabatically arising from the interaction of $\text{Be}^+ + \text{O}^-$ with the O atom initially in its ¹D excited state being

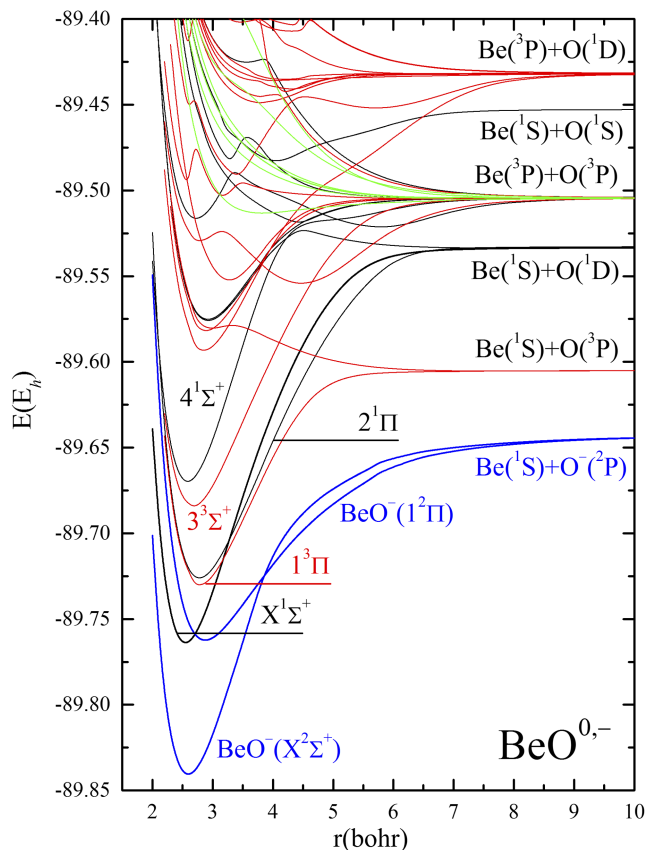


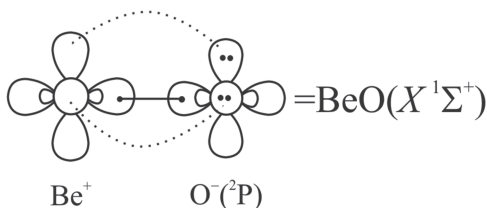
FIG. 1. MRCI potential energy curves of BeO and BeO⁻ (in blue colour).

thus more receptive in the accommodation of a negative charge by $\text{EA}({}^1D) = \text{EA}({}^3P)^{13} + \Delta E({}^1D \leftarrow {}^3P)^{14} = 1.461 + 1.958$ eV = 3.419 eV. A simple classical electrostatic calculation of the dipole moment ($\mu = 2.31$ a.u.) of a pair of charges q separated by $r_e(X^1\Sigma^+) \sim 2.5$ bohr sorts out a $q = 0.92 e^-$ very close to the ideal $\text{Be}^+ + \text{O}^-$ situation. If we want to visualize the major part (“0.77”) of the wavefunction using the

TABLE I. Energies $E(E_h)$, bond distances $r_e(\text{\AA})$, harmonic frequencies $\omega_e(\text{cm}^{-1})$, anharmonic corrections $\omega_e x_e(\text{cm}^{-1})$, adiabatic dissociation energies $D_e(\text{kcal/mol})$, and excitation energies $T_e(\text{cm}^{-1})$ of eleven(two) ${}^4\text{Be}^{16}\text{O}({}^4\text{Be}^{16}\text{O}^-)$ states at the MRCI computational level.

State	-E	r_e	ω_e	$\omega_e x_e$	D_e	T_e
BeO						
$X^1\Sigma^+$	89.764 437	1.346	1446.6	9.9	144.99	0.0
$1^3\Pi$	89.730 514	1.470	1132.6	8.7	78.67	7445
$2^1\Pi$	89.726 401	1.470	1136.6	8.1	121.54	8348
$3^3\Sigma^+$	89.684 680	1.411	1157.2	0.6	113.39	17505
$4^1\Sigma^+$	89.670 354	1.369	1386.0	11.0	104.36	20649
$5^3\Sigma^+$	89.594 102	1.511	1292.3	57.0	101.97	37384
$6^3\Delta$	89.582 446	1.533	1211.1	122.4	49.21	39942
$8^1\Delta$	89.576 097	1.547	921.4	7.1	26.81	41336
$9^1\Sigma^-$	89.575 474	1.543	937.0	13.0	44.83	41473
$10^3\Pi$	89.554 241	2.366	504.2	8.6	31.51	46133
$11^3\Sigma^-$	89.552 527	1.735	958.3	30.7	30.45	46509
BeO ⁻						
$X^2\Sigma^+$	89.845 732	1.376	1397.4	20.2	127.70 ^a	0.0
$1^2\Pi$	89.762 589	1.520 ^a	955.0 ^a	10.9 ^a	75.73 ^a	18248 ^a

^aNo physical significance can be attributed to the calculated energy points above the ground vibrational level of the neutral diatomic. The numerical values provided herein can be considered as Morse parameters.



SCHEME 1.

classical Lewis structures then the valence bond Lewis (vbL) icon depicted in Scheme 1 captures nicely its essence. The oxygen atom is negatively charged in its 2P state while the Be^+ ion is accepting electronic density through the π frame and getting promoted to its 3P state. The “0.77” component of the wavefunction is a σ -bonded system with π migration from O^- to Be^+ , a genuinely closed shell case, while the second (“0.38”) and third (“0.30”) components are open singlet cases due to the 1D atomic ancestral.

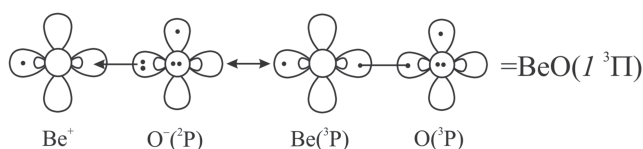
The first excited state ($T_e = 7445 \text{ cm}^{-1}$) is of $^3\Pi$ symmetry dissociating to the ground state fragments $\text{Be}(^1S) + \text{O}(^3P)$. Its equilibrium characteristics are synopsised in $|^3\Pi\rangle \cong 0.97 |1\sigma^2 2\sigma^2 3\sigma^1 1\pi_x^1 1\pi_y^2\rangle$ with the molecular orbitals being practically similar with the ones of the ground state while the atomic populations are $2s^{0.92} 2p_z^{0.39} 2p_x^{0.04} 2p_y^{0.13} /_{\text{Be}} 2s^{1.91} 2p_z^{1.72} 2p_x^{0.95} 2p_y^{1.82} /_{\text{O}}$ ($q_{\text{Be}} = +0.46$). The $\sim +0.5$ Mulliken charge on the Be atom can be interpreted as a mixture of covalent/ionic bonding visualized by the resonant vbL structures of Scheme 2.

There are two triplet coupled electrons, one along the σ frame and located on the Be atom and the other one along the π frame but now “sitting” on the O atom. These two triplet coupled electrons are ready to form two simple bonds.

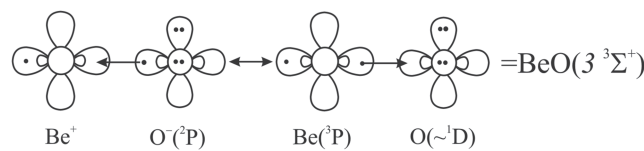
Only one more state, the $^3\Sigma^+$, will be presented as particularly relevant to the purposes of the present work. Its equilibrium CASSCF characteristics are $|^3\Sigma^+\rangle \cong 0.96 |1\sigma^2 2\sigma^1 3\sigma^1 1\pi_x^2 1\pi_y^2\rangle$ and $2s^{0.84} 2p_z^{0.33} 2p_x^{0.14} 2p_y^{0.14} /_{\text{Be}} 2s^{1.86} 2p_z^{0.93} 2p_x^{1.81} 2p_y^{1.81} /_{\text{O}}$ ($q_{\text{Be}} = +0.46$). Once again we can schematically represent the wavefunction with the help of two resonating vbL icons of ionic and covalent origin; see Scheme 3. There is a one electron or half σ bond while another electron is located on the rear side of the Be atom.

The rest of the bound states displayed in Figure 1 are immaterial to the bonding elucidation of the titled species and we will not be concerned with them anymore.

Before we proceed to the discussion of HBeO/BeOH and HBeOH systems, we will present the anionic BeO^- system that is believed to exist due to the large dipole field of the neutral parental system.¹⁵ It is only just a few days ago that the BeO^- species was first detected in a $X^2\Sigma^+(\text{BeO}^-) \rightarrow X^1\Sigma^+(\text{BeO})$ photo detachment experiment by means of



SCHEME 2.



SCHEME 3.

photoelectron velocity map imaging spectroscopy by Mascirotto *et al.*¹⁶ As one can see in Figure 1, there are two BeO^- PECs of $^2\Sigma^+$ and $^2\Pi$ symmetry with their usual molecular constants presented in Table I. It is clear that the $^2\Sigma^+$ state is the ground state of the charged species with a calculated electron affinity (EA) of $\text{EA} = 2.21 \text{ eV}$ (the experimental value is 2.17 eV ¹⁶) while the $^2\Pi$ one is an “excited” state quasi-generate with the $X^1\Sigma^+$ state of the neutral BeO system; see Table I and Figure 1. The CASSCF equilibrium wavefunctions and Mulliken atomic distributions of these two states are

$$|X^2\Sigma^+\rangle \cong 0.96 |1\sigma^2 2\sigma^2 3\sigma^1 1\pi_x^1 1\pi_y^2\rangle,$$

$$2s^{0.76} 2p_z^{0.48} 2p_x^{0.27} 2p_y^{0.27} /_{\text{Be}} 2s^{2.0} 2p_z^{1.72} 2p_x^{1.67} 2p_y^{1.67} /_{\text{O}} (q_{\text{Be}} = +0.13 \text{ and } q_{\text{O}} = -1.13) \text{ and } |^2\Pi\rangle \cong 0.98 |1\sigma^2 2\sigma^2 3\sigma^2 1\pi_x^1 1\pi_y^2\rangle, 2s^{1.48} 2p_z^{0.57} 2p_x^{0.05} 2p_y^{0.11} /_{\text{Be}} 2s^{2.0} 2p_z^{1.78} 2p_x^{0.97} 2p_y^{1.86} /_{\text{O}} (q_{\text{Be}} = -0.28 \text{ and } q_{\text{O}} = -0.72) \text{ with common orbitals being } 1\sigma \cong 2s(\text{O}),$$

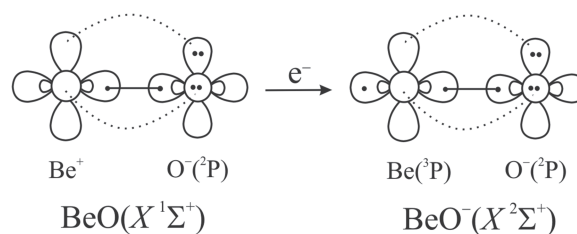
$$2\sigma \cong 0.59 \times 2s(\text{Be}) + 0.53 \times 2p_z(\text{Be}) - 0.82 \times 2p_z(\text{O}),$$

$$3\sigma \cong 0.49 \times 2s(\text{Be}) + 0.32 \times s'(\text{Be}) - 0.49 \times 2p_z(\text{Be}),$$

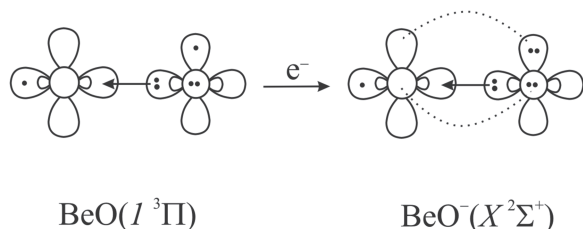
$$1\pi \cong 0.35 \times 2p_\pi(\text{Be}) + 0.87 \times 2p_\pi(\text{O}).$$

At first sight it seems legitimate to consider that the $X^2\Sigma^+(\text{BeO}^-)$ state originates from the $X^1\Sigma^+(\text{BeO})$ one while the $^2\Pi(\text{BeO}^-)$ from $^1\Pi(\text{BeO})$. Both of the above BeO states have a positive charge on the Be atom and this naturally attracts the additional electron. For the formation of the $X^2\Sigma^+(\text{BeO}^-)$ state, we will only consider the “0.77” component of its neutral $X^1\Sigma^+$ ancestor. The minus charge is directed towards the positively charged Be center and hosted into a hybrid orbital pointing away from the O atom; see Scheme 4. The above process neutralizes the Be atom from $+0.76(\text{BeO}, X^1\Sigma^+)$ to $+0.13(\text{BeO}^-, X^2\Sigma^+)$ and thus concentrates the minus charge on O creating a “pseudo” $\text{O}^{2-}(^1S)$ atomic state.

Strangely enough the minus charge does not make the sigma bond shorter as observed in the $\text{Be}_2[r_e(X^1\Sigma_g^+) = 2.477 \text{ \AA}]/\text{Be}_2^- [r_e(X^2\Pi_u/1^2\Sigma_g^+) = 2.223/2.418 \text{ \AA}]$ case¹⁷ through an enhanced polarization of the entailed hybrid orbitals. The equilibrium distance of BeO^- , $r_e(X^2\Sigma^+) = 1.376 \text{ \AA}$, is somewhere between the $r_e[\text{BeO}(X^1\Sigma^+)] = 1.346 \text{ \AA}$ and $r_e[\text{BeO}(^1\Pi)] = 1.470 \text{ \AA}$ and this bond elongation can be rationalized due to



SCHEME 4.

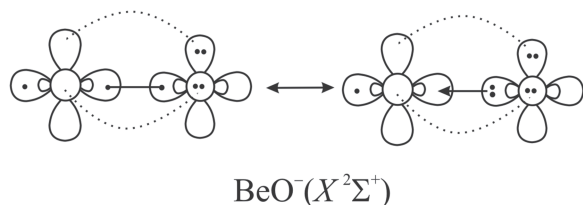


SCHEME 5.

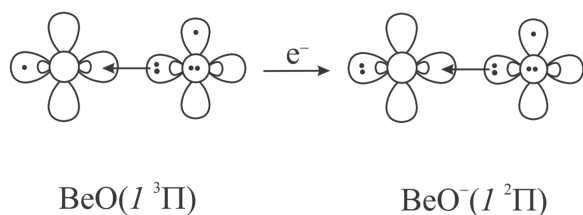
the participation/resonance of two ($X^1\Sigma^+$ and $1^3\Pi$) neutral states in the ground anionic one. If we consider the $1^3\Pi(\text{BeO})$ state, then the addition of the minus charge to a $2p_\pi$ O orbital creates an “unstable” $\text{O}^{2-}(^1\text{S})$ atom stabilized in a $^2\Sigma^+$ BeO^- environment; see Scheme 5. Certainly both BeO^- vBL Schemes 4 and 5 look similar but there is a difference in the sigma frame. In the vBL diagram visualizing the $\text{BeO}(X^1\Sigma^+) + e^- \rightarrow \text{BeO}^-(X^2\Sigma^+)$ process there is a “traditional” two electron sigma bond between the Be and O⁻ atoms, while in the second alternative “route,” i.e., $\text{BeO}(1^3\Pi) + e^- \rightarrow \text{BeO}^-(X^2\Sigma^+)$, there is a “dative bond” or in other words a sigma electron migration from the electron rich O^{2-} to the electron deficient Be^+ center. So the $\text{BeO}^-(X^2\Sigma^+)$ state can be characterized as a resonance situation as shown in Scheme 6.

The $^2\Pi$ state originates from the $1^3\Pi$ neutral state by grafting the minus charge to the $2s2p_z$ hybrid orbital located on the positively charged Be atom; see Scheme 7. The minus charge is now singlet coupled to the singly occupied 3σ electron of the parental neutral state while the spin defining electron is now “sitting” on O. So the BeO^- system can potentially exist in two different states with the spin defining electron in either a $\sigma(\text{Be})$ or $\pi(\text{O})$ orbital and it is chemically bound and not trapped by the dipole moment of the ionic $\text{Be}^+\text{O}^- X^1\Sigma^+$ ground state.¹⁵ The PECs of these two symmetries cross at 3.85 bohr (see Figure 1) and the spin orbit interaction of the $\Omega = 1/2$ states ($^2\Sigma_{1/2}^+$ and $^2\Pi_{1/2}$) is only 40 cm^{-1} . Their non adiabatic behavior is negligible (less than 1 cm^{-1}) for all vibrational levels of its ground $X^2\Sigma^+$ state up to the ground neutral vibrational level ($X^1\Sigma^+, v=0$).

Having analyzed the electronic structure of both the neutral and anionic species, we are now in a position to understand the electronic and geometrical structure of their hydrogenated products, i.e., $\text{HBeO}^{0,-}$, BeOH , and HBeOH . There is a recent



SCHEME 6.



SCHEME 7.

and vivid interest in the HBeO/BeOH system; see Refs. 8 and 18–24. The stablest isomer of the $[\text{HBeO}]$ ensemble is beryllium monohydroxide, $\text{BeOH}(\tilde{X}^2A')$, a system that is being said to “... exhibits somewhat incompatible structure and bonding.”¹⁸ According to the latest state-of-the-art *ab initio* calculations, the adiabatic BeOH angle is predicted to be 141.2° but the barrier to linearity is extremely small, just $\Delta E = 129 \text{ cm}^{-1}$,¹⁸ thus classifying the triatomic as a floppy or quasilinear system, a fact recently confirmed experimentally by Mascaritolo *et al.*²⁰ It is rather peculiar though how such a triangular geometry is so floppy, so the question of why this is happening naturally arises.

On the other hand, the HBeO isomer in its $\tilde{X}^2\Pi$ state is perfectly linear with no tendency to bend, is strongly bound with respect to either $\text{H}(^2\text{S}) + \text{BeO}(1^3\Pi)$ or $\text{HBe}(X^2\Sigma^+) + \text{O}(^3\text{P})$, lies above the global $\text{BeOH}(\tilde{X}^2A')$ minimum by $11\,917 \text{ (MRCI)/13\,057 (RCCSD(T)) cm}^{-1}$, and has an isomerization barrier (HBeO/BeOH) of $10\,920 \text{ cm}^{-1}$ with respect to the $\text{HBeO}(\tilde{X}^2\Pi)$ minimum.²²

Finally, the HBeOH system in its $\tilde{X}^1A'(C_s)$ state exhibits a BeOH angle of 139° (present work) similar to the one found in $\text{BeOH}(\tilde{X}^2A')$ and is pretty much bound with dissociation energies ranging from 74 to 149 kcal/mol depending on the reaction path.⁸

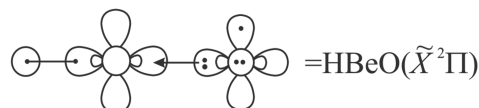
Let us consider first the HBeO system that was extensively studied by Zaidi *et al.*²² in 2006. Its $\tilde{X}^2\Pi$ and $\tilde{I}^2\Sigma^+$ states present no mystery regarding their bonding pattern. Their MRCI equilibrium characteristics are $|\tilde{X}^2\Pi\rangle \cong 0.98 |1\sigma^2 2\sigma^2 3\sigma^2 1\pi_x^1 1\pi_y^2\rangle$ and $|\tilde{I}^2\Sigma^+\rangle \cong 0.98 |1\sigma^2 2\sigma^2 3\sigma^1 1\pi_x^1 1\pi_y^2\rangle$ with $1\sigma \cong 2s(\text{O})$, $2\sigma \cong 0.62 \times 2s(\text{Be}) + 0.52 \times 2p_z(\text{Be}) + 0.80 \times 1s(\text{H})$, $3\sigma \cong 0.35 \times 2s(\text{Be}) - 0.47 \times 2p_z(\text{Be}) + 0.93 \times 2p_z(\text{O})$, and $1\pi \cong 0.30 \times 2p_\pi(\text{Be}) + 0.90 \times 2p_\pi(\text{O})$.

It is obvious even from the geometrical features that $\text{HBeO}(\tilde{X}^2\Pi, r_e(\text{BeO}) = 1.475 \text{ \AA})$ (see Scheme 8) is formed from the $\text{BeO}(1^3\Pi, r_e = 1.470 \text{ \AA})$ state while $\text{HBeO}(\tilde{I}^2\Sigma^+, r_e(\text{BeO}) = 1.415 \text{ \AA})$ from the $\text{BeO}(3^3\Sigma^+, r_e = 1.414 \text{ \AA})$ one (see Scheme 9), although the latter state correlates adiabatically to $\text{H}(^2\text{S}) + \text{BeO}(X^1\Sigma^+)$; see also Figure 1 of Ref. 22. Now, let us move to the more mysterious quasilinear BeOH species. In order to unveil its bonding scenario, we have considered that a $\text{H}(^2\text{S})$ atom can attack BeO either along its σ ($X^1\Sigma^+$ or $3^3\Sigma^+$) or its π frame ($1^3\Pi$). We have optimized the linear $\text{BeOH}(^2\Sigma^+)$, perpendicular $\text{BeOH}(^2A'(\theta = 90^\circ))$, and adiabatic equilibrium structures $\text{BeOH}(^2A'(\theta \cong 140^\circ))$. The results are indeed revealing,

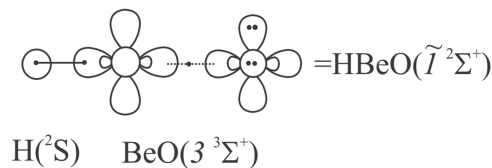
$$|^2\Sigma^+(\text{or } ^2A'(\theta = 180^\circ))\rangle \cong 0.98 |1\sigma^2 2\sigma^2 3\sigma^1 1\pi_x^1 1\pi_y^2\rangle$$

with $2\sigma \cong 0.33 \times 2s(\text{Be}) - 0.37 \times 2p_z(\text{Be}) + 0.76 \times 2p_z(\text{O}) - 0.78 \times 1s(\text{H})$, $3\sigma \cong -0.78 \times 2s(\text{Be}) - 0.58 \times 2p_z(\text{O})$, and $1\pi \cong 0.30 \times 2p_\pi(\text{Be}) + 0.90 \times 2p_\pi(\text{O})$,

$$|^2A'(\theta = 90^\circ)\rangle \cong 0.98 |1a^2 2a^2 3a^2 4a^1 1a'^2\rangle$$



SCHEME 8.



SCHEME 9.

with $2a' \cong -0.49 \times 2s(\text{Be}) - 0.50 \times 2p_z(\text{Be}) + 0.87 \times 2p_z(\text{O})$, $3a' \cong 0.75 \times 2p_y(\text{O}) + 0.75 \times 1s(\text{H})$, $4a' \cong 0.77 \times 2s(\text{Be}) - 0.60 \times 2p_z(\text{Be})$, and $1a'' \cong 0.30 \times 2p_x(\text{Be}) + 0.90 \times 2p_x(\text{O})$, and finally

$$|\tilde{X}^2A'(\theta \cong 140^\circ)\rangle \cong 0.98 |1a'^2 2a'^2 3a'^2 4a'^1 1a''^2\rangle$$

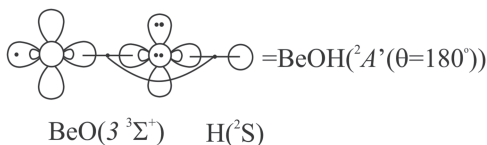
with $2a' \cong 0.38 \times 2s(\text{Be}) - 0.40 \times 2p_z(\text{O}) + 0.79 \times 2p_z(\text{O}) - 0.68 \times 1s(\text{H})$, $3a' \cong 0.85 \times 2p_y(\text{O}) + 0.37 \times 1s(\text{H})$, $4a' \cong 0.78 \times 2s(\text{Be}) + 0.59 \times 2p_z(\text{Be})$, and $1a'' \cong 0.30 \times 2p_x(\text{Be}) + 0.90 \times 2p_x(\text{O})$.

The $^2A'(\theta = 180^\circ$ and $90^\circ)$ wavefunctions are graphically transcribed in Schemes 10 and 11.

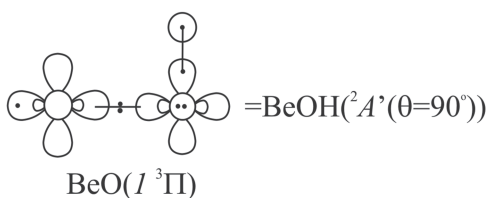
The $\text{BeOH}(^2\Sigma^+)$ dissociates adiabatically to $\text{BeO}(X^1\Sigma^+) + \text{H}(^2S)$ but it connects diabatically to $\text{BeO}(3^3\Sigma^+) + \text{H}(^2S)$ while $\text{BeOH}(^2A'(\theta = 90^\circ))$ dissociates to $\text{BeO}(1^3\Pi) + \text{H}(^2S)$, so it can be said that the building blocks are the $1^3\Pi$ and $3^3\Sigma^+$ BeO states. These states are energetically apart by 46 mE_h (see Table I) while their hydrogenated products differ by $\sim 10 \text{ mE}_h$. This means that within the BeOH environment the two BeO states, $1^3\Pi$ and $3^3\Sigma^+$, are being stabilized by $\sim 35 \text{ mE}_h$ and since they are of the same symmetry label under C_s geometry, they both heavily interact to build the $\text{BeOH}(\tilde{X}^2A')$ molecule. In other words, the ground \tilde{X}^2A' state of BeOH is a resonance, a “quantum mixture” of both $\text{BeOH}(^2\Sigma^+)$ and $\text{BeOH}(^2A'(\theta = 90^\circ))$ “chemical patterns.” Their geometrical characteristics are indeed apocalyptic.

The $\theta_{\text{BeOH}(\tilde{X}^2A')} = 139.6^\circ \cong \frac{\theta_{\text{BeOH}(^2\Sigma^+)} + \theta_{\text{BeOH}(^2A'(\theta=90^\circ))}}{2}$ ($= 135^\circ$) while $r_{\text{BeO}(\tilde{X}^2A')} = 1.404 \text{ \AA} \cong \frac{r_{\text{BeO}(^2\Sigma^+)} + r_{\text{BeO}(^2A'(\theta=90^\circ))}}{2}$ ($= 1.414 \text{ \AA}$). This means that schematically the \tilde{X}^2A' is captured by the resonance shown in Scheme 12 that explains the non rigidity of the OH bond or the non locality of the H atom being at the same time along and perpendicular to the BeO axis, an eloquent manifestation of the quantum nature of matter.

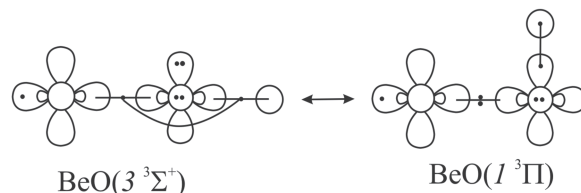
The spin defining electron, localized on the rear side of the Be atom, is ready to form another bond. And this is indeed the case. By approaching a $\text{H}(^2S)$ atom we get the \tilde{X}^1A' HBeOH state. Our MRCI optimized geometry reveals its connection to the \tilde{X}^2A'



SCHEME 10.



SCHEME 11.

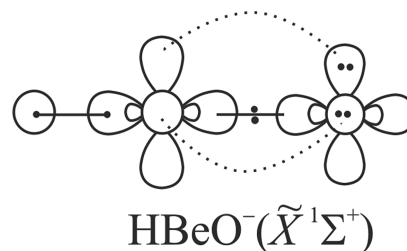


SCHEME 12.

BeOH parental state, i.e., $r(\text{HBe}) = 1.333 \text{ \AA}$, $r(\text{BeO}) = 1.408 \text{ \AA}$, $r(\text{OH}) = 0.948 \text{ \AA}$, $\angle \text{HBeO} = 176.88^\circ$, and $\angle \text{BeOH} = 138.86^\circ$, $E = -91.093\,544 \text{ E}_h$. The BeOH angle in HBeOH is practically identical to the one in BeOH, revealing that way the resonance of the $\text{BeO } 1^3\Pi$ and $3^3\Sigma^+$ building blocks. The tetratomic though is not floppy since its linear $\text{HBeOH}(^1\Sigma^+)$ structure lies $\sim 10 \text{ mE}_h$ above the actual ground state geometry. So, in both $\text{BeOH}(\tilde{X}^2A')$ and $\text{HBeOH}(\tilde{X}^1A')$ the H atom of the hydroxyl group has a non locality in space, being at the same time along the BeO axis and perpendicular to it, while its average position is at the midway between these two forms, i.e., $\angle \text{BeOH} \approx 140^\circ$.

Now let us consider the HBeO^- species. It can be viewed as arising from either $\text{BeO}^-(X^2\Sigma^+) + \text{H}$ or $\text{HBeO}(\tilde{X}^2\Pi) + e^-$. Its ground state is the linear HBeO^- structure of $^1\Sigma^+$ symmetry with no tendency to bend and with equilibrium structural parameters of $r(\text{HBe}) = 1.388 \text{ \AA}$, $r(\text{BeO}) = 1.378 \text{ \AA}$, and $E = -90.489\,463 \text{ E}_h$ and thus with an electron affinity value of $\text{EA} = 2.90 \text{ eV}$ with respect to $\text{HBeO}(\tilde{X}^2\Pi)$. The vBL icon that captures the character of the anion is shown in Scheme 13.

Having understood the diatomics BeO and BeO^- , we are now in a position to tackle the $\text{BeOBe}^{+,0,-}$ species that are hypervalent according to the traditional rules of valence and whose binding is “. . .not easily rationalized using simple molecular orbital concepts.”^{1,8} Before entering into the bonding analysis, we should remind the major points of BeOBe. First, its highly multireference ground $\tilde{X}^1\Sigma_g^+$ state is practically degenerate with its first excited state of $\tilde{a}^3\Sigma_u^+$ symmetry and of single reference character and second, although the bonding mechanism is still puzzling, the charge distribution points to something like $\text{Be}^+\text{O}^{2-}\text{Be}^+$. It is certainly strange how two closed shell fragments, BeO and Be, create a quite stable closed shell molecule where all electrons are singlet coupled but at the same time a triplet spin state, i.e., a pair of electrons initially singlet coupled turned out to be triplet coupled, is practically degenerate to the singlet one. Moreover, due to the inversion symmetry both Be atoms should be *in situ* in identical atomic states within BeOBe. The best way to understand how a molecular species is formed is through its evolution in the configuration space and not simply through isolated energy point calculations. So the natural way to study BeOBe is through the interaction of $\text{BeO} + \text{Be}$. In Table II we gather the molecular constants of the $\tilde{X}^1\Sigma_g^+$ and $\tilde{a}^3\Sigma_u^+$



SCHEME 13.

BeOBe states, practically identical in nature, that hint at the same binding pattern and at the somehow equivalency of the triplet and singlet coupled electrons. Their equilibrium configurations are

$$|\tilde{X}^1\Sigma_g^+\rangle \cong |1\sigma_g^2 1\sigma_u^2 [0.73 \times (2\sigma_g^2) - 0.64 \times (2\sigma_u^2)] 1\pi_{u,x}^2 1\pi_{u,y}^2\rangle,$$

$$|\tilde{a}^3\Sigma_u^+\rangle \cong 0.98 |1\sigma_g^2 1\sigma_u^2 2\sigma_g^2 2\sigma_u^1 1\pi_{u,x}^2 1\pi_{u,y}^2\rangle,$$

with $1\sigma_u \cong -0.44[2s(\text{Be}_L) - 2s(\text{Be}_R)] - 0.48[2p_z(\text{Be}_L) + 2p_z(\text{Be}_R)] + 0.84 \times 2p_z(\text{O})$, $2\sigma_g \cong 0.57[2s(\text{Be}_L) + 2s(\text{Be}_R)] - 0.38[2p_z(\text{Be}_L) - 2p_z(\text{Be}_R)]$, $2\sigma_u \cong 0.53[2s(\text{Be}_L) - 2s(\text{Be}_R)] - 0.46[2p_z(\text{Be}_L) + 2p_z(\text{Be}_R)]$, $1\pi_u \cong 0.27[2p_\pi(\text{Be}_L) + 2p_\pi(\text{Be}_R)] + 0.84 \times 2p_\pi(\text{O})$ and Mulliken atomic distributions $2s^{0.97} 2p_z^{0.44} 2p_x^{0.11} 2p_y^{0.11} /_{\text{Be}_{L,R}} 2s^{1.84} 2p_z^{1.26} 2p_x^{1.70} 2p_y^{1.70} /_{\text{O}} (q_{\text{Be}_{L,R}} = +0.28, q_{\text{O}} = -0.56)$.

We should remind at this point that the $\tilde{X}^1\Sigma_g^+$ state is considered as multiconfiguration in character due to the “0.73” and “0.64” components; see also Refs. 1 and 8. The $1\sigma_u$ orbital is a “bonding” combination of the $2p_z(\text{O})$ atomic orbital with two “bonding” $2s2p_z$ hybrids located on each Be atom while the $2\sigma_g$ and $2\sigma_u$ when properly localized²⁵ reveal two Be $2s2p_z$ hybrids pointing outwards and thus being complementary to the “bonding” ones. The electrons of these $2\sigma_g/2\sigma_u$ hybrids are either singlet (as in $\tilde{X}^1\Sigma_g^+$) or triplet (as in $\tilde{a}^3\Sigma_u^+$) coupled. Considering their small energy gap, $\Delta E(\tilde{a}^3\Sigma_u^+ \leftarrow \tilde{X}^1\Sigma_g^+) = 265 \text{ cm}^{-1}$ (see Table II), we conclude that the singlet spin coupling does not provide any substantial binding. Based also on the Hurley, Lennard–Jones, Pople transformation,²⁵ we can see that the $\tilde{X}^1\Sigma_g^+$

state is not multiconfiguration in nature as previously stated (see, e.g., Ref. 8) but a single reference one with a total weight of $\sqrt{0.73^2 + 0.64^2} = 0.97$ exactly as in the $\tilde{a}^3\Sigma_u^+$ one. Two configurations are needed in order to describe correctly the open singlet character of the terminal electrons as in the GVB–PP way of thinking. The final piece of the puzzle, the key element of how/why two “closed shell” fragments, BeO and Be, create a stable BeOBe species, is provided by the PECs that capture the BeO + Be interaction. In Figure 2, we display PECs of $1A_1(C_{2v})$ symmetry along the BeO + Be reaction coordinate at the CASSCF level. It is clear that the 9th state of purely ionic character, i.e., $\text{BeO}^-(X^2\Sigma^+) + \text{Be}^+(^2S)$, transcends its nature to all states below. The PEC of the $\tilde{X}^1\Sigma_g^+$ state feels an abrupt change at ~ 5.0 bohr, an avoided crossing initiated from the $\text{BeO}^-(X^2\Sigma^+) + \text{Be}^+(^2S)$ asymptote. Putting together all these elements, we conclude that the bonding in both the $\tilde{X}^1\Sigma_g^+$ and $\tilde{a}^3\Sigma_u^+$ states is covalent in nature but the constituent atoms are found *in situ* in their ionized Be^+ and O^{2-} states; see Scheme 14. The O atom is “trapped” inside the BeOBe species in its unstable $\text{O}^{2-}(^1S)$ state. The two $2p_z(\text{O})$ electrons are spread along the σ frame of the molecule into the empty “bonding” $2s2p_z$ hybrids of the two Be^+ atoms that are sequentially neutralized with a synchronous depopulation of the negatively overloaded O atom. This σ delocalization “pushes” the $\text{Be}^+(^2S)$ electrons in the opposite direction that are either singlet ($\tilde{X}^1\Sigma_g^+$) or triplet ($\tilde{a}^3\Sigma_u^+$) coupled. There is also some small π delocalization. The Mulliken distributions are quite revealing. Every Be^+ gets an additional charge of 0.41 (σ frame) + 0.11×2 (π frame) e^- from a

TABLE II. Molecular constants of $\text{BeOBe}(\tilde{X}^1\Sigma_g^+/\tilde{a}^3\Sigma_u^+)$, $\text{BeOBe}^{+/-}(\tilde{X}^2\Sigma_g^+/\tilde{X}^2\Sigma_u^+)$, $\text{BeOBeH}(\tilde{X}^2\Sigma^+)$, $\text{HBeOBeH}(\tilde{X}^1\Sigma_g^+)$, and $\text{BeOBeH}^{+/-}(\tilde{X}^1\Sigma^+)$ at the MRCI computational level.

$\text{BeOBe}(\tilde{X}^1\Sigma_g^+)$
$r_e(\text{BeO}) = 1.410 \text{ \AA}$, $E = -104.550\,789 \text{ E}_h$, $\omega_{b,ss,as} = 129, 1062, 1467 \text{ cm}^{-1}$ ^a
$\text{BeOBe}(\tilde{a}^3\Sigma_u^+)$
$r_e(\text{BeO}) = 1.410 \text{ \AA}$, $E = -104.549\,582 \text{ E}_h$, $\omega_{b,ss,as} = 133, 1038, 1437 \text{ cm}^{-1}$ ^b
$\text{BeOBe}^+(\tilde{X}^2\Sigma_g^+)$
$r_e(\text{BeO}) = 1.397(1.398) \text{ \AA}$, $E = -104.252\,644(-104.258\,015) \text{ E}_h$ ^c
$r_e(\text{BeO}) = 1.463$ and 1.348 \AA , $E = -104.253\,740 \text{ E}_h$ ^d
$\text{BeOBe}^-(\tilde{X}^2\Sigma_u^+)$
$r_e(\text{BeO}) = 1.422 \text{ \AA}$, $E = -104.592\,916 \text{ E}_h$ ^e
$r_e(\text{BeO}) = 1.469$ and 1.387 \AA , $E = -104.576\,233 \text{ E}_h$ ^f
$\text{BeOBeH}(\tilde{X}^2\Sigma^+)$
$r_e(\text{BeO}) = 1.408(1.408)$ and $1.414(1.414) \text{ \AA}$, $E = -105.195\,443(-105.205\,865) \text{ E}_h$ ^g
$\text{HBeOBeH}(\tilde{X}^1\Sigma_g^+)$
$r_e(\text{BeO}) = 1.408(1.411) \text{ \AA}$, $E = -105.829\,030(-105.855\,882) \text{ E}_h$ ^g
$\text{BeOBeH}^+(\tilde{X}^1\Sigma^+)$
$r_e(\text{BeO}) = 1.468(1.468)$ and $1.344(1.345) \text{ \AA}$, $E = -104.897\,061(-104.905\,023) \text{ E}_h$ ^g
$\text{BeOBeH}^-(\tilde{X}^1\Sigma^+)$
$r_e(\text{BeO}) = 1.449(1.462)$ and $1.397(1.392) \text{ \AA}$, $E = -105.212\,396(-105.238\,396) \text{ E}_h$ ^g

^a $\omega_b(\text{ending})$, $s(\text{symmetric})$ $s(\text{treching})$, $a(\text{asymmetric})$ $s(\text{treching})$ at the CISD computational level.

^b $\omega_b(\text{ending})$, $s(\text{symmetric})$ $s(\text{treching})$, $a(\text{asymmetric})$ $s(\text{treching})$ at the RCCSD(T) computational level.

^cResults in parentheses at the RCCSD(T) level.

^dSymmetry broken structure at the MRCI computational level, the stability of the centrosymmetric equilibrium geometry has been checked at the RCCSD(T) level along the asymmetric stretching coordinate, see Ref. 26 for details.

^eRCCSD(T) computational level.

^fSymmetry broken structure at the MRCI computational level.

^gMRCI(RCCSD(T)) results.

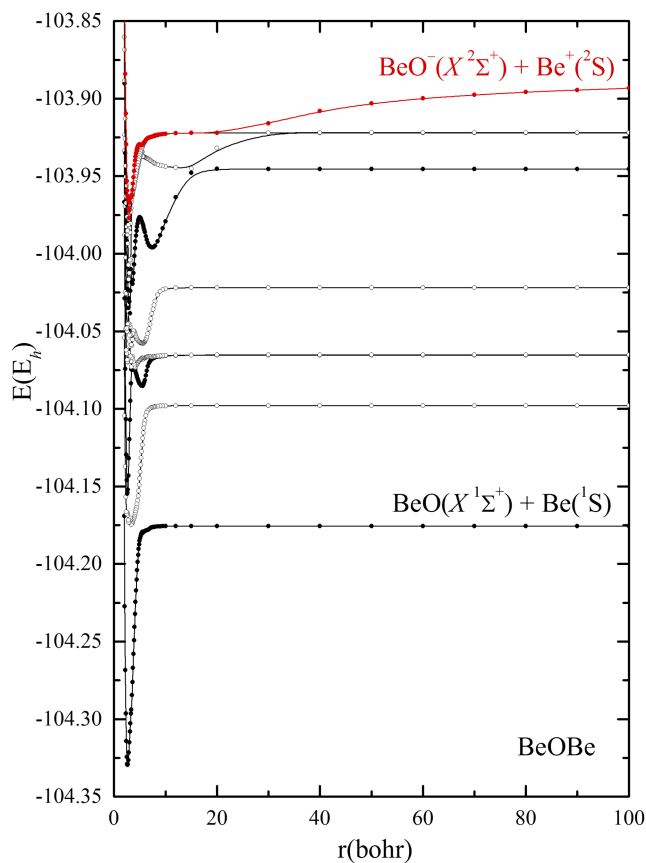
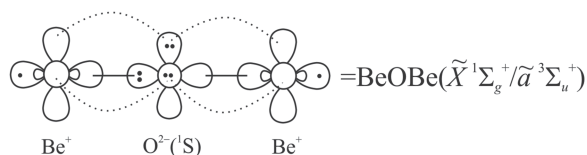


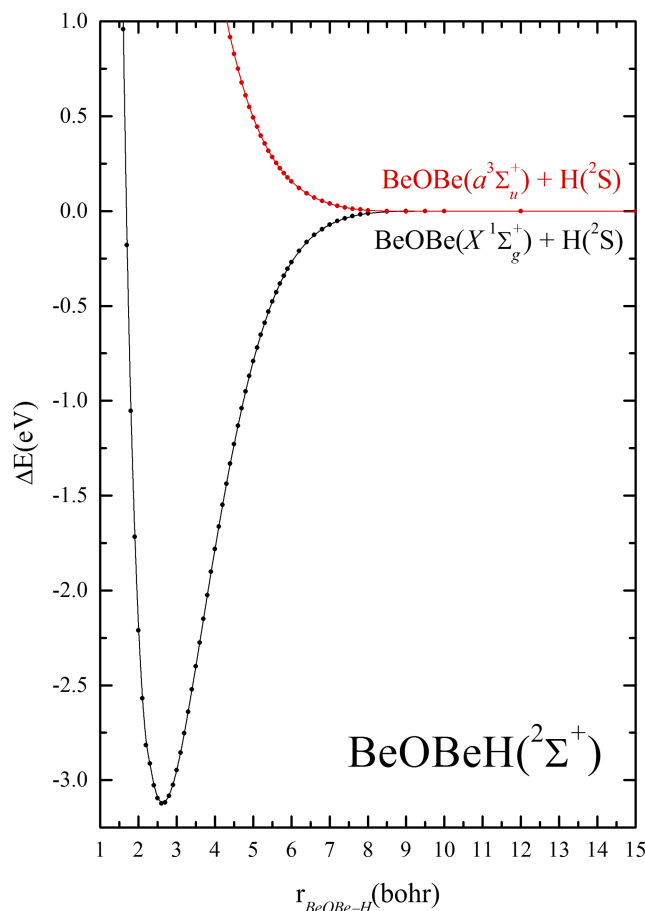
FIG. 2. CASSCF potential energy curves of the BeO + Be interaction.

$2s^{2.0}2p_z^{2.0}2p_x^{2.0}2p_y^{2.0}$ O dianion. We can even say that since the σ and π delocalizations do not entail any spin decoupling process the two Be atoms are “buttoned” to O through the $\text{Be}^+\text{O}^{2-}\text{Be}^+$ diabats with the two remaining electrons pointing outwards and being immaterial to the bonding. The latter is also in compliance with the identical molecular constants of the two quasidegenerate states; see Table II.

The simplest thing to do in order to monitor their behavior is to attach one and/or two $\text{H}(^2\text{S})$ atoms. The approach of a H atom creates a stable $\text{BeOBeH}(\tilde{X}^2\Sigma^+)$ species through the formation of a σ BeH bond; see Figure 3. The spin defining electron is localized on a sp_z orbital pointing in the opposite direction of the H atom. The formation of a BeH sigma bond does not distort the equilibrium characteristics of the $\text{BeOBe}(\tilde{X}^1\Sigma_g^+)$ species due to the nature of the BeOBe bonds, i.e., $r_{\text{BeO}}(\tilde{X}^1\Sigma_g^+) = 1.410 \text{ \AA}$ versus $r_{\text{BeO}}(\tilde{X}^2\Sigma^+) = 1.408$ and 1.414 \AA , see Table II. Moreover, the $\text{BeOBe}(\tilde{X}^1\Sigma_g^+) + \text{H}(^2\text{S}) \rightarrow \text{BeOBeH}(\tilde{X}^2\Sigma^+)$ process is accompanied by an energy stabilization of 4.05 eV at the RCCSD(T) computational level. The Mulliken population analysis is quite revealing, $\text{Be}_L(2s^{1.0}2p_z^{0.49}2p_x^{0.09}2p_y^{0.09}) \text{O}(2s^{1.84}2p_z^{1.21}2p_x^{1.76}2p_y^{1.76}) \text{Be}_R(2s^{0.66}2p_z^{0.47}2p_x^{0.07}2p_y^{0.07}) \text{H}(1s^{1.23})$. It shows that the BeOBe



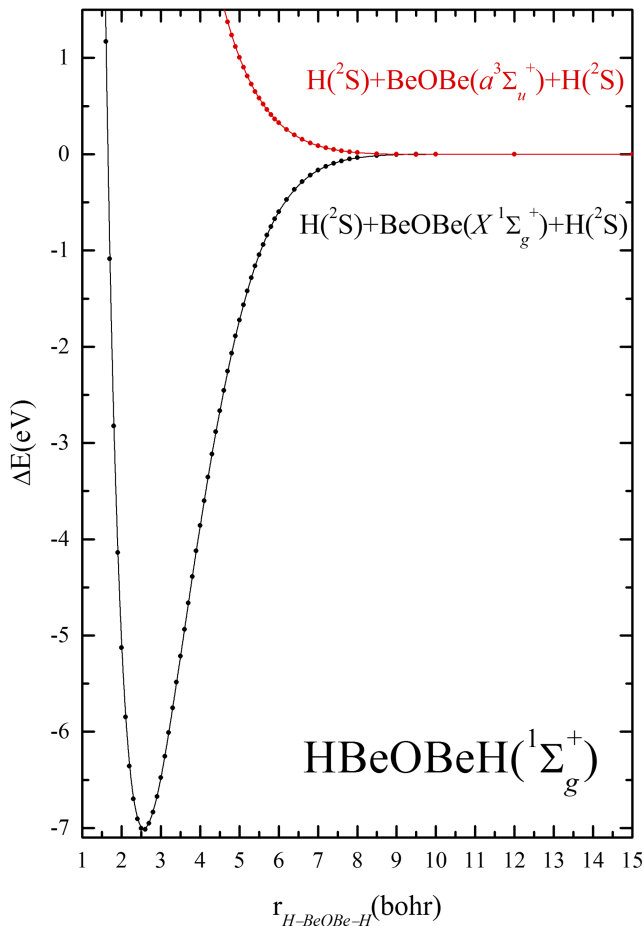
SCHEME 14.

FIG. 3. CASSCF potential energy curves of $\text{BeOBeH}(\tilde{X}^2\Sigma^+)$.

system stays quasi intact with the exception of some sigma migration to the H atom from its closest Be atom. The addition of a second $\text{H}(^2\text{S})$ atom is not a surprise since it forms another sigma bond with the $\bullet\text{BeOBeH}(\tilde{X}^2\Sigma^+)$ spin defining electron; see Figure 4. As previously, the equilibrium characteristics of $\text{BeOBe}(\tilde{X}^1\Sigma_g^+)$ remain essentially the same (see Table II) due to the dative nature of the $\text{Be} \leftarrow \text{O} \rightarrow \text{Be}$ bonds. The second sigma HBe bond, i.e., $\text{BeOBeH}(\tilde{X}^2\Sigma^+) + \text{H}(^2\text{S}) \rightarrow \text{HBeOBeH}(\tilde{X}^1\Sigma_g^+)$, amounts to 4.08 eV (RCCSD(T) level) energetically equal to the first sigma BeH bond ($D_e = 4.05 \text{ eV}$). Each Be atom has a Mulliken atomic distribution of $2s^{0.71}2p_z^{0.60}2p_x^{0.08}2p_y^{0.08}$ due to a sigma electronic migration to the H atoms. The formation of both $\text{BeOBeH}(\tilde{X}^2\Sigma^+)$ and $\text{HBeOBeH}(\tilde{X}^1\Sigma_g^+)$ proceeds through $\text{BeOBe}(\tilde{a}^3\Sigma_u^+) + \text{H}(^2\text{S})$ or $+(\text{H}(^2\text{S}) + \text{H}(^2\text{S}))$ via an avoided crossing with the $\text{BeOBe}(\tilde{X}^1\Sigma_g^+) + \text{H}(^2\text{S})$ or $+(\text{H}(^2\text{S}) + \text{H}(^2\text{S}))$ adiabatic channels, respectively, due to the spin decoupling/recoupling mechanism. It can also be said that the $\text{HBeOBeH}(\tilde{X}^1\Sigma_g^+)$ species is formed by $\text{HBe}^+(\text{X}^1\Sigma^+) + \text{O}^{2-}(\text{^1S}) + \text{Be}^+(\text{X}^1\Sigma^+)$; see Scheme 15. The unstable $\text{O}^{2-}(\text{^1S})$ is stabilized when two $\text{BeH}^+(\text{X}^1\Sigma^+)$ units approach and “buttoned” to $\text{O}^{2-}(\text{^1S})$ via σ and π delocalizations.

Another thing we can do is to remove or add an electron in order to create $\text{BeOBe}^+(\tilde{X}^2\Sigma_g^+)$ (IE = 8.113 eV, present work) or $\text{BeOBe}^-(\tilde{X}^2\Sigma_u^+)$ (EA = 0.98 eV, present work), respectively. Their equilibrium wavefunctions and Mulliken populations are

$$|\tilde{X}^2\Sigma_g^+(\text{BeOBe}^+)\rangle \cong 0.97 |1\sigma_g^2 1\sigma_u^2 2\sigma_g^1 1\pi_{u,x}^2 1\pi_{u,y}^2\rangle$$

FIG. 4. CASSCF potential energy curves of HBeOBeH($1\Sigma_g^+$).

with

$$1\sigma_u \cong -0.67[2s(\text{Be}_L) - 2s(\text{Be}_R)] - 0.70[2p_z(\text{Be}_L) + 2p_z(\text{Be}_R)] + 0.84 \times 2p_z(\text{O}),$$

$$2\sigma_g \cong 0.87[2s(\text{Be}_L) + 2s(\text{Be}_R)] - 0.51[2p_z(\text{Be}_L) - 2p_z(\text{Be}_R)],$$

$$1\pi_u \cong 0.42[2p_\pi(\text{Be}_L) + 2p_\pi(\text{Be}_R)] + 0.85 \times 2p_\pi(\text{O})$$

and

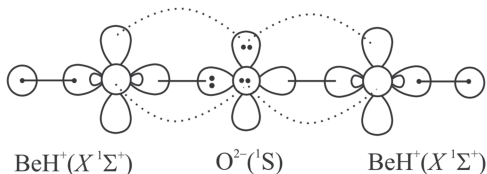
$$2s^{0.83}2p_z^{0.30}2p_x^{0.13}2p_y^{0.13}/_{\text{Be}_{L,R}}2s^{1.84}2p_z^{1.23}2p_x^{1.66}2p_y^{1.66}/\text{O}$$

and

$$\begin{aligned} & \left\{ \tilde{X}^2\Sigma_u^+(\text{BeOBe}^-) \right\} \\ & \cong \left| 1\sigma_g^2 1\sigma_u^2 [0.91 \times (2\sigma_g^2) - 0.17 \times (3\sigma_g^2)] 2\sigma_u^1 1\pi_{u,x}^2 1\pi_{u,y}^2 \right\} \\ & + 0.31 \left| 1\sigma_g^2 1\sigma_u^2 2\sigma_g^1 3\sigma_g^1 2\sigma_u^1 1\pi_{u,x}^2 1\pi_{u,y}^2 \right\} \end{aligned}$$

with

$$1\sigma_u \cong -0.61[2s(\text{Be}_L) - 2s(\text{Be}_R)] - 0.66[2p_z(\text{Be}_L) + 2p_z(\text{Be}_R)] + 0.83 \times 2p_z(\text{O}),$$



SCHEME 15.

$$2\sigma_g \cong 0.59[2s(\text{Be}_L) + 2s(\text{Be}_R)] + 0.40[s'(\text{Be}_L) + s'(\text{Be}_R)] - 0.36[2p_z(\text{Be}_L) - 2p_z(\text{Be}_R)] + 0.42 \times s'(\text{O}),$$

$$3\sigma_g \cong -0.90[s'(\text{Be}_L) + s'(\text{Be}_R)] - 0.53[2p_z(\text{Be}_L) + 2p_z(\text{Be}_R)] - 1.12 \times s'(\text{O}),$$

$$2\sigma_u \cong -0.69[2s(\text{Be}_L) - 2s(\text{Be}_R)] + 0.62[2p_z(\text{Be}_L) + 2p_z(\text{Be}_R)] - 0.16 \times 2p_z(\text{O})$$

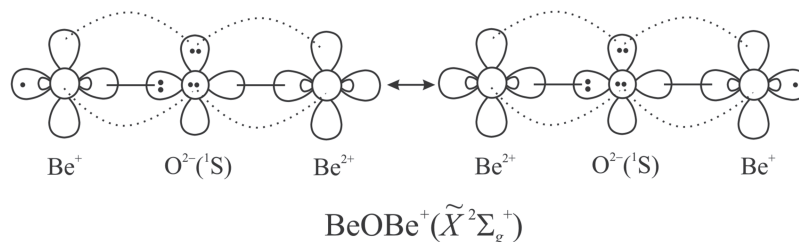
$$1\pi_u \cong 0.37[2p_\pi(\text{Be}_L) + 2p_\pi(\text{Be}_R)] + 0.85 \times 2p_\pi(\text{O}),$$

and

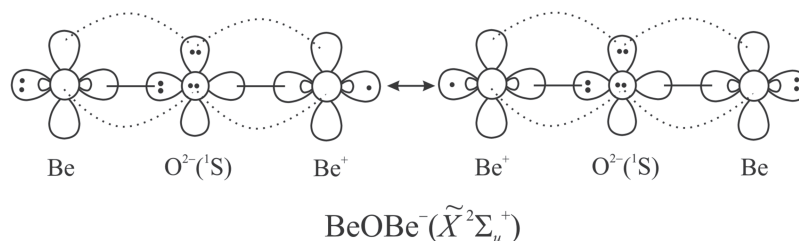
$$2s^{1.09}2p_z^{0.52}2p_x^{0.11}2p_y^{0.11}/_{\text{Be}_{L,R}}(2s + s')^{2.42}2p_z^{1.29}2p_x^{1.71}2p_y^{1.71}/\text{O}.$$

When properly read, they reveal the same chemical pattern as the one found in the neutral BeOBe($\tilde{X}^1\Sigma_g^+/\tilde{a}^3\Sigma_u^+$) species. It is interesting to talk about the wavefunction of the anionic triatomic. There are three main configurations with coefficients of “0.91,” “−0.17,” and “0.31” and one may conclude that it is of multiconfiguration character. This is not so if we properly read these configurations. The first two, i.e., “0.91” and “−0.17,” can be written as a GVB–PP wavefunction if we use the Hurley, Lennard–Jones, and Pople transformation²⁵ while the third one (“0.31”) is based on the same Hartree product as above but multiplies the second spin function that couples three electrons in a doublet. Thus, we have a common Hartree orbital product that multiplies the two spin functions that couple three electrons into a doublet. In a pictorial way the above cationic and anionic wavefunctions are shown in Schemes 16 and 17. It is obvious from these vBL schemes that the electron is either removed from or added to the $2s2p_z$ hybrid of the Be(L or R) center with the σ/π bonds being practically intact (see molecular constants in Table II). But there is one major difference between the charged (+/−) and the neutral (0) BeOBe species. There are two resonating vBL structures with a localized + or − charge centered either on the left or right Be atoms and this makes the charged BeOBe $^{+,-}$ species prone to symmetry breaking if not properly treated.²⁶ We have optimized both symmetrical ($D_{\infty h}$) and non symmetrical structures ($C_{\infty v}$); see Table II. It is legitimate to ask if a second electron can be added to the BeOBe $^-(\tilde{X}^2\Sigma_u^+)$ species. We have tested that possibility but the resulting dianion is not stabler than the anion. We strongly believe though that longer $-(\text{BeOBe}^-)_n$ chains can accommodate a second electron.

The spin defining electron of both $\tilde{X}^2\Sigma_g^+(\text{BeOBe}^+)$ and $\tilde{X}^2\Sigma_u^+(\text{BeOBe}^-)$ states is clearly ready to form a sigma bond with an incoming H atom; see Figures 5 and 6, respectively. When a H atom is present, the “g/u” symmetry is lost and the spin defining electron will eventually be localized on the Be atom facing H. This means that there should be an interaction between the $\tilde{X}^2\Sigma_g^+/\tilde{A}^2\Sigma_u^+(\text{BeOBe}^+)$ and $\tilde{X}^2\Sigma_u^+/\tilde{A}^2\Sigma_g^+(\text{BeOBe}^-)$ states in order to break their centrosymmetric character, localize the electron on one Be end, and eventually form the BeH bond. And this is indeed what happens as clearly displayed in Figures 5 and 6. The molecular constants of both BeOBeH $^{+,-}(\tilde{X}^1\Sigma^+)$ species reveal some interesting features. First, the addition of the H atom, $(\text{BeOBe}^{+,-} + \text{H}(2S)) \rightarrow \text{BeOBeH}^{+,-}$ or in other words the strength of the resulting BeH bond, is $D_e = 4.00$ (BeOBeH $^+$) and 3.96 (BeOBe $^-$) eV, practically the same as the one in BeOBeH(4.05 eV) and



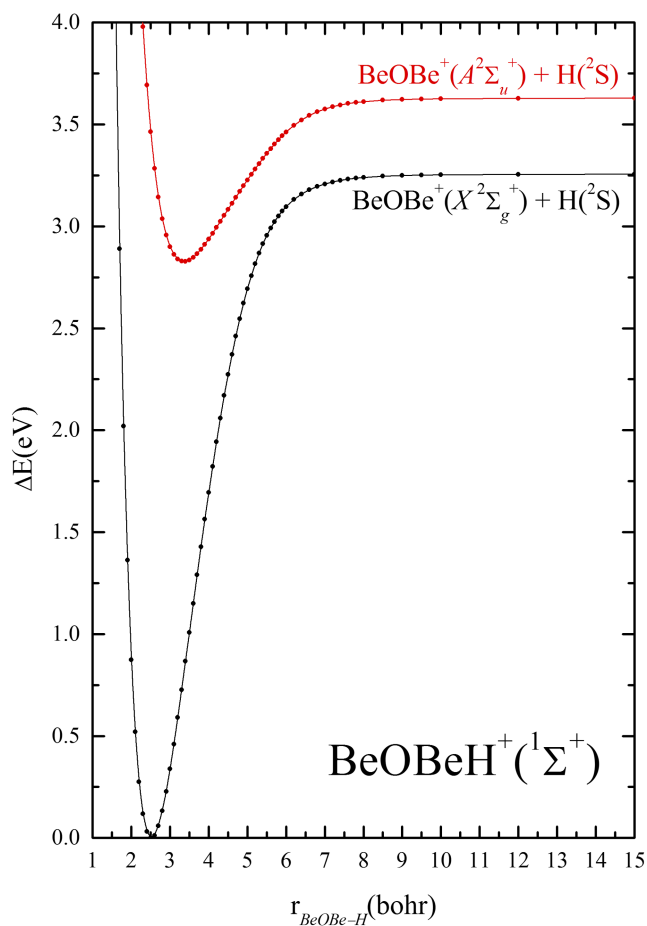
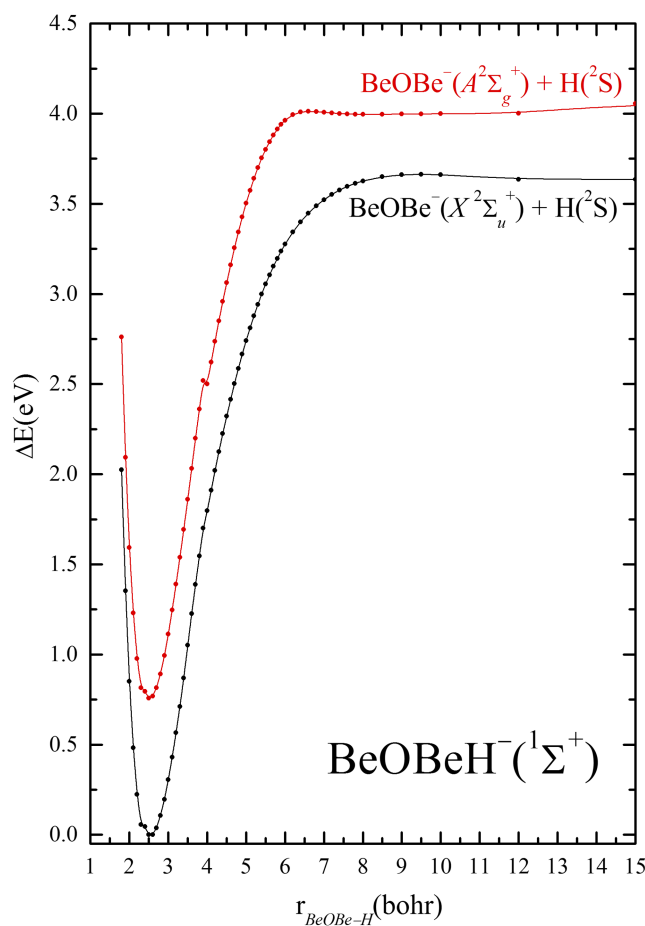
SCHEME 16.



SCHEME 17.

HBeOBeH(4.08 eV) in agreement with the dative nature of the Be←O→Be bonds. Second, the BeOBe unit in both BeOBeH^{+,-} systems equilibrates in a geometry that is practically the same as the symmetry broken one of the parental BeOBe^{+,-} systems (see Table II). And this is an expected outcome of the H presence whose role is to bifurcate the $D_{\infty h}$ equilibrium of the charged

species. It is not a surprise that the addition of one or two H atoms to the neutral BeOBe retains its structure while its (H) addition to BeOBe^{+,-} destroys the interference of the two resonating vBL structures (see Schemes 16 and 17) or in other words the vBL structures are now quantum decoherent due to the interaction with H.

FIG. 5. CASSCF potential energy curves of BeOBeH⁺(¹Σ⁺).FIG. 6. CASSCF potential energy curves of BeOBeH⁻(¹Σ⁺).

III. CONCLUDING REMARKS

With the aim to understand the bonding in Be containing molecules, we have studied $\text{BeO}^{0,-}$ and $\text{BeOBe}^{+,0,-}$ along with their hydrogenated products like $\text{HBeO}^{0,-}$, BeOH , HBeOH , $\text{BeOBeH}^{+,0,-}$, and HBeOBeH . We have discussed in some detail the $\text{BeO}(X^1\Sigma^+, 1^3\Pi, 3^3\Sigma^+)$ and $\text{BeO}^-(X^2\Sigma^+, 1^2\Pi)$ states being the building stones for $\text{BeOBe}^{+,0,-}$ and their hydrogenated products. The most important features of the current work are the following:

1. The ground $\text{BeO } X^1\Sigma^+$ state is a σ bonded system with partial π migration between Be^+ and O^- ions, while the $1^3\Pi$ and $3^3\Sigma^+$ states can be viewed as resonance cases in which Be participates as Be^+ and $\text{Be}(^3P)$.
2. The $\text{BeO}^- X^2\Sigma^+$ state is a chemically bound anion with an EA = 2.21 eV and with a binding pattern based on the resonance/participation of both $\text{BeO}(X^1\Sigma^+) + e^- \rightarrow \text{BeO}^-(X^2\Sigma^+) \leftarrow \text{BeO}(1^3\Pi) + e^-$ processes.
3. The quasi linear $\text{BeOH}(\tilde{X}^2A')$ species is due to the resonance of $\text{BeOH}(^2A'(\theta = 180^\circ))$ and $\text{BeOH}(^2A'(\theta = 90^\circ))$ structures that result from $\text{BeO}(3^3\Sigma^+)$ and $\text{BeO}(1^3\Pi)$, respectively. The adiabatic equilibrium value of its angle ($\sim 140^\circ$) is very close to the median of the above limiting geometries (linear and L-shaped) conferring a nonlocality to the H atom.
4. The BeOBe system in both its quasi degenerate $\tilde{X}^1\Sigma_g^+$ and $\tilde{a}^3\Sigma_u^+$ states is due to a σ and partial π electronic migration between an “unstable” $\text{O}^{2-}(^1S)$ dianion and two Be^+ cations. There are two electrons at the end sides that are either singlet or triplet coupled. Their small energy separation means that their spin coupling is immaterial to the nature of the formed BeO bonds. The spin defining electrons can be coupled with either one or two H atoms or with an “incoming” electron creating that way the $\text{BeOBe}^-(\tilde{X}^2\Sigma_u^+)$ state bound by EA = 0.98 eV. The strength of the BeH bonds is practically the same (~ 4.0 eV) across the $\text{BeOBeH}^{+,0,-}$ and HBeOBeH series of molecules.
5. The species studied herein exist just because the constituent atoms can be present in more than their ground states or in other words their excited states participate in the bonding process. Similarly, molecular fragments can participate in a resonant way within larger entities. So, as a conclusion we can say that there is nothing wrong with the Lewis rules of valence provided that we do not forget that excited states play a protagonist role in bond

formation or in other words the usual rules of valency can equally well be applied to the excited states of the constituent fragments.

- ¹M. C. Heaven, V. E. Bondybey, J. M. Merritt, and A. L. Kaledin, *Chem. Phys. Lett.* **506**, 1 (2011).
- ²L. P. Theard and D. L. Hildenbrand, *J. Chem. Phys.* **41**, 3416 (1964).
- ³C. A. Thompson and L. Andrews, *J. Chem. Phys.* **100**, 8689 (1994).
- ⁴L. Andrews, G. V. Chertihin, C. A. Thompson, J. Dillon, S. Byrne, and C. W. Bauschlicher, Jr., *J. Phys. Chem.* **100**, 10088 (1996).
- ⁵J. M. Merritt, V. E. Bondybey, and M. C. Heaven, *J. Phys. Chem. A* **113**, 13300 (2009).
- ⁶I. O. Antonov, B. J. Barker, and M. C. Heaven, *J. Chem. Phys.* **134**, 044306 (2011).
- ⁷B. Ostojić, P. Jensen, P. Schwerdtfeger, B. Assadollahzadeh, and P. R. Bunker, *J. Mol. Spectrosc.* **263**, 21 (2010).
- ⁸A. I. Boldyrev and J. Simons, *J. Phys. Chem.* **99**, 15041 (1995).
- ⁹A. S. Ivanov, I. A. Popov, A. I. Boldyrev, and V. V. Zhidankin, *Angew. Chem., Int. Ed.* **53**, 9617 (2014).
- ¹⁰T. H. Dunning, Jr., *J. Chem. Phys.* **90**, 1007 (1989).
- ¹¹H.-J. Werner, P. J. Knowles, G. Knizia, F. R. Manby, M. Schütz, P. Celani, W. Györfy, D. Kats, T. Korona, R. Lindh, A. Mitrushenkov, G. Rauhut, K. R. Shamasundar, T. B. Adler, R. D. Amos, A. Bernhardsson, A. Berning, D. L. Cooper, M. J. O. Deegan, A. J. Dobbyn, F. Eckert, E. Goll, C. Hampel, A. Hesselmann, G. Hetzer, T. Hrenar, G. Jansen, C. Köppl, Y. Liu, A. W. Lloyd, R. A. Mata, A. J. May, S. J. McNicholas, W. Meyer, M. E. Mura, A. Nicklaß, D. P. O’Neill, P. Palmieri, D. Peng, K. Pflüger, R. Pitzer, M. Reiher, T. Shiozaki, H. Stoll, A. J. Stone, R. Tarroni, T. Thorsteinsson, and M. Wang, *MOLPRO* version 2015.1, a package of *ab initio* programs, 2015, see <http://www.molpro.net>.
- ¹²T. E. Sorensen and W. B. England, *Int. J. Quantum Chem.* **76**, 259 (2000).
- ¹³W. Chaibi, R. J. Peláez, C. Blondel, C. Drag, and C. Delsart, *Eur. Phys. J. D* **58**, 29 (2010).
- ¹⁴A. Kramida, Yu. Ralchenko, J. Reader, and NIST ASD Team, *NIST Atomic Spectra Database (Version 5.3)* (National Institute of Standards and Technology, Gaithersburg, MD, 2015), <http://physics.nist.gov/asd>.
- ¹⁵K. D. Jordan and R. Seeger, *Chem. Phys. Lett.* **54**, 320 (1978); Y. Yoshioka and K. D. Jordan, *J. Chem. Phys.* **73**, 5899 (1980); *Chem. Phys.* **56**, 303 (1981).
- ¹⁶K. J. Mascaritolo, A. R. Dermer, M. L. Green, A. M. Gardner, and M. C. Heaven, *J. Chem. Phys.* **146**, 054301 (2017).
- ¹⁷A. Kalemos, *J. Chem. Phys.* **145**, 214302 (2016).
- ¹⁸J. Koput, *J. Comp. Chem.* **38**, 37 (2017).
- ¹⁹I. F. C. Mbapeh, S. C. G. Kempf, and P. Jensen, *J. Phys. Chem. A* **119**, 10112 (2015).
- ²⁰K. J. Mascaritolo, J. M. Merritt, M. C. Heaven, and P. Jensen, *J. Phys. Chem. A* **117**, 13654 (2013).
- ²¹M. Vasiliiu, D. Feller, J. L. Gole, and D. A. Dixon, *J. Phys. Chem. A* **114**, 9349 (2010).
- ²²A. Zaidi, S. Lahmar, Z. Ben Lakhdar, P. Rosmus, and G. Chambaud, *Chem. Phys.* **321**, 41 (2006).
- ²³J. Koput and K. A. Peterson, *J. Phys. Chem. A* **107**, 3981 (2003).
- ²⁴C. W. Bauschlicher, Jr., S. R. Langhoff, and H. Partridge, *J. Chem. Phys.* **84**, 901 (1986).
- ²⁵A. C. Hurley, J. E. Lennard-Jones, and J. A. Pople, *Proc. R. Soc. A* **220**, 446 (1953).
- ²⁶A. Kalemos, *J. Chem. Phys.* **138**, 224302 (2013); **144**, 234315 (2016).